Available online at www.sciencedirect.com
ScienceDirect
Journal of Power Sources 159 (2006) 1015–1024
JOURNAL OF POWER SOURCES
www.elsevier.com/locate/jpowsour

# Nanocomposite membranes of surface-sulfonated titanate and Nafion® for direct methanol fuel cells

Chang Houn Rhee [a], Youngkwon Kim [b], Jae Sung Lee [b,c,*], Hae Kyung Kim [d], Hyuk Chang [d]

[a] *Corporate R&D, Research Park, LG Chem Ltd., Daejeon 305-380, Republic of Korea*
[b] *School of Environmental Engineering, Pohang University of Science and Technology, Pohang 790-784, Republic of Korea*
[c] *Department of Chemical Engineering, Pohang University of Science and Technology, Pohang 790-784, Republic of Korea*
[d] *Materials and Device Laboratory, Samsung Advanced Institute of Technology, Suwon 440-600, Republic of Korea*

Received 24 October 2005; received in revised form 6 December 2005; accepted 6 December 2005
Available online 18 January 2006

**Abstract**

Various thiol and sultone groups were grafted onto the surface of titanate nanosheets to render organic sulfonic acid ($HSO_3$–) functionality. The nanocomposite membranes were cast together with Nafion® using these materials as inorganic fillers. Nanocomposite membranes containing surface-sulfonated titanates showed higher proton conductivity than composite membranes containing untreated $TiO_2$ P25 particles. They showed better mechanical and thermal stability than Nafion alone. The methanol permeability of nanocomposite membranes decreased with increasing the content of the sulfonated titanate in the nanocomposite membranes. The relative permeability of methanol through these composite membranes with 2 and 5 M methanol solutions was reduced by up to 38 and 26%, respectively, relative to pristine Nafion 115 membranes. The membrane electrode assembly using Nafion/sulfonated titanate nanocomposite membranes exhibited up to 57% higher power density than the assembly containing a pristine Nafion membrane under typical operating conditions of direct methanol fuel cells.


*Keywords:* Sulfonic acid groups; Nafion; Nanocomposite membranes; Methanol crossover; Direct methanol fuel cells

## 1. Introduction

Among various fuel cells, direct methanol fuel cells (DMFCs) are suited for portable devices or transportation applications owing to their high energy density at low operating temperatures and ease of handling a liquid fuel [1]. Yet they have major technical drawbacks, i.e. slow oxidation kinetics of methanol and high methanol crossover from the anode to the cathode [2–4]. In particular, the high methanol permeation through Nafion® membranes significantly lowers fuel efficiency and cell performance, and thus impedes the commercial development of DMFCs. The methanol crossover is dictated by the polymer electrolyte membrane, which is employed to provide proton conduction from the anode to the cathode and effective separation of the anode (methanol) and cathode (oxygen) reactants. Nafion® membrane is by far the most studied proton electrolyte membrane for DMFCs as well as polymer electrolyte membrane (PEM) fuel cells.

Nafion® membranes are chemically inert in both oxidizing and reducing atmospheres of the fuel cell, have demonstrated a long term stability under fuel cell operating conditions, and have an excellent proton conductivity (0.07–0.23 S $cm^{-1}$) [5]. Yet the high methanol permeability rate across the membrane poses a critical problem in realization of DMFC for practical use [6]. This phenomenon is caused by protonic drag of methanol, similar to electro-osmotic drag of water. Methanol is easily transported together with solvated protons by means of the electro-osmotic drag as well as by diffusion through the water-filled ion channels within the Nafion® structure and through the Nafion® itself. Methanol transported across the membrane is chemically oxidized to $CO_2$ and water at the cathode, and causes a loss in coulombic efficiency for methanol consumption as much as 20% under practical operational conditions [7].

* Corresponding author. Tel.: +82 54 279 2266; fax: +82 54 279 5528.
*E-mail address:* jlee@postech.ac.kr (J.S. Lee).

0378-7753/$ – see front matter © 2005 Elsevier B.V. All rights reserved.
doi:10.1016/j.jpowsour.2005.12.006

There have been many attempts to reduce the methanol permeability through the polymer electrolyte membranes: (i) to treat the surface of the membranes to block the methanol transport, (ii) to control the size of the proton transport channels using different block copolymers and cross-linkage, (iii) to develop new types of electrolyte polymers and (iv) to introduce a winding pathway for a methanol by making a composite with inorganic fillers. The composite membranes have been mostly prepared by addition of non-conductive ceramic oxide such as silica, titania, zirconia, mixed silicon–titanium oxides, zeolites, silicon–aluminum oxides and montmorillonite in the Nafion® membrane [8–15]. Zirconium phosphates [16–21] have also been examined, which have a moderate proton conductivity when humidified ($\sim 10^{-3}$ S cm$^{-1}$) [16]. Among the reported zirconium phosphate fillers, γ-layered zirconium phosphates containing sulfophenyl group had the highest conductivity ($\sim 0.05$ S cm$^{-1}$) at 373 K and 95% relative humidity (RH) [19]. The main focus in these works was to obtain the electrolyte membrane operating at higher temperatures over 373 K. When applied to DMFC, these composite membranes containing inorganic moieties indeed reduced the methanol crossover. Yet this effect did not always lead to a desired improvement in the performance of the membrane–electrode assembly (MEA), mainly because the proton conductivity of the composite membranes containing these less proton conductive oxides was markedly lowered compared with that of a pristine Nafion® membrane.

In order to minimize the loss of proton conductivity caused by adding the inorganics, while reducing the methanol permeability, we modified the surface of titanate nanosheets with an organic sulfonic acid group and formed a nanocomposite electrolyte membrane with Nafion®. The synthesized titanate is a layer-structured material that has a large surface area of over 500 m$^2$ g$^{-1}$ and its proton form ($H^+$-titanate) has a proton conductivity of $2.66 \times 10^{-6}$ S cm$^{-1}$ at 573 K [22]. An organic species bearing the functionality ($HSO_3$– group) was grafted onto the surface of the titanate nanosheets. This is the method commonly employed to render strong acidity to minerals like kaolinite, magadiite and montmorillonite [23–26]. The characteristics of the nanocomposite electrolyte membrane were studied in terms of methanol crossover, proton conductivity, tensile strength and spectroscopic properties. Although the proton conductivity was slightly lowered, the nanocomposite membranes exhibited improved performance by reducing the methanol crossover and enhancing the mechanical strength compared with a pristine Nafion 115 membrane.

## 2. Experimental

### 2.1. Preparation of titanate nanosheets

Titanate nanosheets were synthesized according to the method described in detail elsewhere [27,28]. Thus, titanium oxysulfate ($TiOSO_4 \cdot xH_2SO_4 \cdot xH_2O$, Aldrich) was used as a titanium source, in which the $TiO_2$ content was 33.6 wt% (estimated by thermogravimetric analysis at 1073 K). In a typical synthesis, titanium oxysulfate powder and deionized water were placed in a beaker, and then this mixture was uniformly slurried under ambient conditions. An aqueous ammonia solution (28–30 wt%, J.T. Baker) was added slowly to prevent the slurried mixture from boiling over during the hydroxylation reaction between titanium oxysulfate and ammonia. The molar composition of $TiOSO_4 \cdot xH_2SO_4 \cdot xH_2O$, $NH_4OH$, and $H_2O$ in the mixture was 1:5:50. The mixed solution was transferred into a Teflon-lined autoclave and statically heated in an oven at 393 K for 3 days. After the hydrothermal treatment, the formed white precipitates were filtered out, washed thoroughly with deionized water until the pH of the washing solution reached around 7 and then subsequently washed with absolute ethanol. The wet products were dried in an oven at 353 K for 24 h to obtain white ammonium titanate [$(NH_4)_2Ti_3O_{7-x}N_x$] powders.

### 2.2. Functionalization of titanate nanosheets

Titanate nanosheets were treated with 1N $H_2SO_4$ at 300 K to convert ammonium titanate [$(NH_4)_2Ti_3O_{7-x}N_x$] into hydrogen titanate ($H_2Ti_3O_{7-x}N_x$, $H^+$-titanate). The surface functionalization of $H^+$-titanate was performed using the surface hydroxyl groups of titanate by condensation with 3-mercaptopropyltrimethoxy silane (3-MPTMS) and 3-mercaptopropyldimethoxymethyl silane (3-MPDMS) or dehydration with 1,3-propane sultone (1,3-PS) and 1,4-butane sultone (1,4-BS) as sulfonic acid precursors. The reactions were carried out at the refluxing temperature of toluene (383 K) for 24 h with the molar ratio of $H^+$-titanate, sulfonic acid precursor and toluene of 1:0.5:15. In case of thiol precursors (3-MPTMS and 3-MPDMS), the thiol (–SH) group grafted onto titanate was oxidized into sulfonic acid ($HSO_3$–) with 10 wt% hydrogen peroxide at 333 K and then treated with 1N $H_2SO_4$ at ambient temperature for complete protonation [29]. The prepared samples were separated by filtration, washed with deionized water and ethanol, and dried at 353 K in a vacuum oven. On the other hand, sultone precursors (1,3-PS and 1,4-BS) directly gave the sulfonic acid group from ring opening of sultone and did not need further treatments after the surface functionalization of titanate. Scheme 1 summarizes these functionalization steps using these precursors. Functionalized samples were denoted by HS-titanate (precursor) or $HSO_3$-titanate (precursor) as indicated.

### 2.3. Fabrication of composite membranes

To prepare a nanocomposite membrane, a desired amount of prepared $HSO_3$-titante was added into 5 wt% Nafion solution (DuPont), and then stirred mechanically and degassed by ultrasonication. The contents of functionalized titanates in the mixture were varied in 3, 5, 7 and 10 wt% based on Nafion. The prepared mixture was slowly poured into a glass dish in an amount that would give a thickness of ca. 120 μm at the formed nanocomposite membrane. The filled glass dish was placed on the leveled plate of a vacuum dry oven, and then was dried by slowly increasing the temperature from 353 to 403 K to prevent crevice formation of the composite membrane. Finally, the residual solvent in the nanocomposite membrane was fully removed by evacuation at 403 K for 12 h. The recast nanocomposite membranes were boiled at 353 K in 10 wt% hydrogen peroxide and

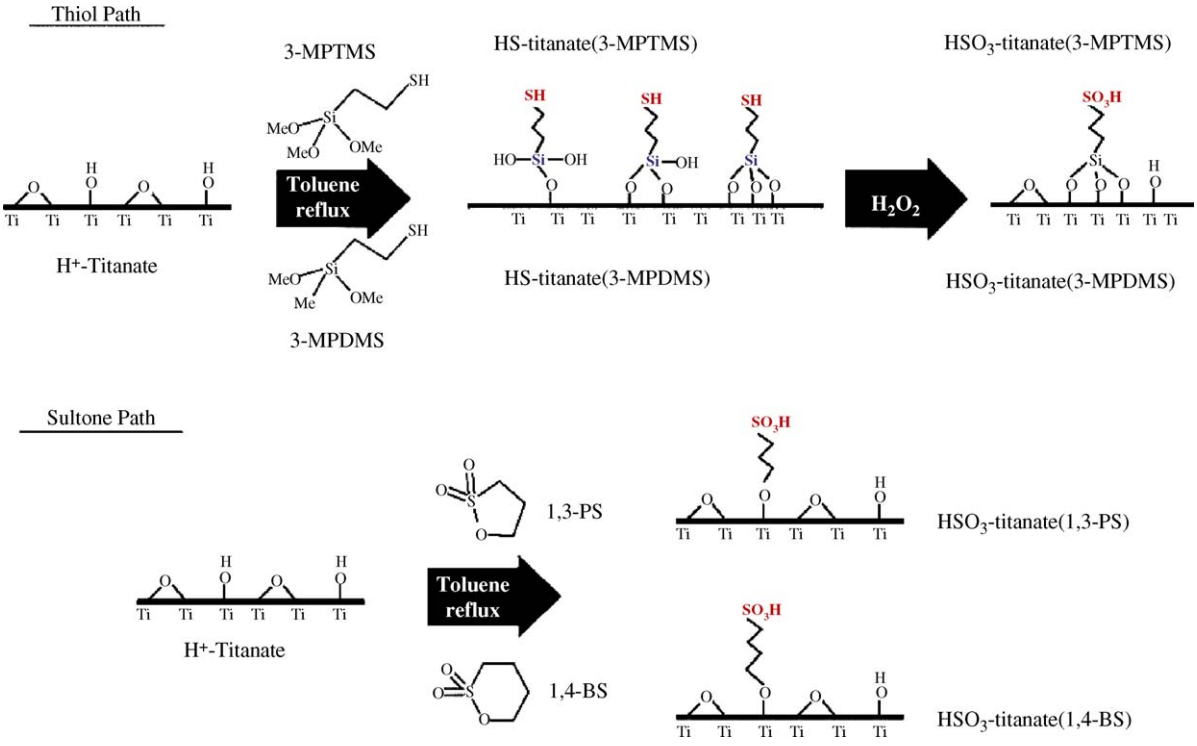


Scheme 1. A schematic representation for the functionalization steps of nanostructured titanates.

rinsed with deionized water. Finally, the obtained nanocomposite membrane was converted into the $H^+$-form by immersing it in 1N $H_2SO_4$ solutions for several hours at 353 K, and rinsing repeatedly with deionized water to remove the excess acid.

### 2.4. Physical characterization

X-ray diffraction (XRD) patterns were obtained on a MAC Science Co., M18XHF diffractometer with Cu Kα radiation (40 kV, 200 mA). The thermal properties of functionalized (HS– or $HSO_3$–) titanates were analyzed by thermogravimetric analysis (TGA, TGS-2). The TGA analyzer was operated in the range of 323–1073 K at a heating rate of 10 K $min^{-1}$ under air flow of 60 ml $min^{-1}$. The thiol (HS–) or sulfonic ($HSO_3$–) groups were analyzed by X-ray photoelectron spectra (XPS) acquired with a VG-Scientific ESCALAB 220 iXL spectrometer equipped with a hemispherical electron analyzer and Mg Kα (1253.6 eV) X-ray source. The $^{29}$Si solid-state NMR measurements were performed on a Varian Unity Inova 300 MHz spectrometer (7.4 T) equipped with a 7 mm Chemagnetics MAS probe head using a sample rotation rate of 5.5 kHz. Tetramethylsilane (TMS) was used as the chemical shift standard for $^{29}$Si (0 ppm). The spectra of $^{29}$Si MAS NMR were measured at a frequency of 59.590 MHz.

### 2.5. Ion exchange capacity measurements

The ion-exchange capacity (IEC) (mmol of sulfonic acid/g of $HSO_3$-titanate) of each sample was determined by the back-titration method. Thus, 0.5 g of the sample was soaked overnight in 50 ml of distilled water containing 5 ml of 0.1N NaOH to exchange sodium ions with the protons in the inorganic. Back-titration was accomplished by titrating the remaining NaOH in solution with 0.1N HCl solutions. The IEC values were obtained by subtracting the added volume of 0.1N HCl from the initial 0.1N NaOH volume.

### 2.6. Methanol permeability measurements

The methanol permeability of the composite membranes was measured at 300 K in a single cell without electrodes. The membrane permeate side was dry by flowing He gas (30 ml $min^{-1}$) and the opposite side was wet by flowing 2 or 5 M methanol/water solution (1 ml $min^{-1}$). The amounts of methanol and water that crossed through the membrane were determined by a gas chromatography (GC, HP 6890) equipped with a packed column (Porapak Q) and a thermal conductivity detector (TCD).

### 2.7. Ionic conductivity measurements

The ionic conductivity of the composite membranes was measured by a four-point probe method using an ac impedance analyzer. The composite membrane was fixed in a measuring cell made of two outer platinum foils and two inner platinum wires. The installed cell was placed in a chamber with controlled humidity and temperature. By applying constant currents ($I$) through the two outer Pt-probes and measuring voltage drops ($V$) across the two inner Pt-probes, the resistance ($R$) of the membrane was measured. The ionic conductivity ($\sigma$) was calculated by $\sigma = L/(A \times R)$, where $L$ and $A$ are the distance between the two inner Pt-probes and the cross-sectional area of the membrane, respectively. The impedance measurements were carried

out in the frequency region from 0.1 to 105 Hz and in the ac current amplitude of 1 mA using electrochemical impedance analyzer (EG&G 263A Potentiostat/Galvanostat, FRD 100 frequency response detector) with Powersuite (v2.53) Software.

### 2.8. Tensile strength measurements

To measure the tensile strength, a nanocomposite membrane was cut into the testing size (5 mm × 5 cm). The prepared test specimen was installed into an Instron 4206 instrument for tensile strength measurements at a crosshead speed of 5 mm $min^{-1}$.

### 2.9. Performance tests for a single cell

The catalyst slurries for cathode and anode were prepared by mixing Pt black and Pt–Ru black with 5 wt% Nafion solutions, respectively. For fabrication of the membrane–electrode assembly (MEA), the catalyst slurry was coated on carbon paper employed as an electrode substrate. The catalyst loading was approximately 8 mg $cm^{-1}$ for both anode and cathode and the effective electrode area of the single cell was 10 $cm^2$. The MEA was fabricated by hot pressing anode/membrane/cathode layers at 398 K and 3500 psi for 5 min. The performance of the single cell with this MEA was evaluated at 313 K with 2 M methanol/water solution and air supplied into the anode and cathode sides of the single cell, respectively.

## 3. Results and discussion

### 3.1. Synthesis and characterization of sulfonated titanate nanosheets

The synthesis and characterization of titanate nanosheets have been discussed in detail elsewhere [28]. In this work, this nanosheet was used as the base material for surface functionalization by organic sulfonic acid groups.

The ion-exchange capacity (IEC, mmol of sulfonic acid/g of $HSO_3$-titanate) is an important factor determining ion conductivity. Thus IEC of each sample was determined by the back-titration method as described in Section 2 and the results are shown in Fig. 1. The $H^+$-titanate treated with 1N $H_2SO_4$ had neutral pH of 7.4 and IEC of 0.526 mmol $g^{-1}$, which represents that ammonium ions in the interlayer of as-synthesized titanate were exchanged with $H^+$. In case of 3-MPTMS as a grafting precursor, the resulting $HSO_3$-titanate (3-MPTMS) had a lower pH and a higher IEC value. On the other hand, $HSO_3$-titanate (1,4-BS) had similar pH and IEC values as $H^+$-titanate, indicating that sufficient surface functionalization was not accomplished by using 1,4-BS. However, the resulting $HSO_3$-titanate (3-MPTMS), $HSO_3$-titanate (3-MPDMS) and $HSO_3$-titanate (1,3-PS) samples had at least ca. 2 times higher IEC values than that of $H^+$-titanate.

In Fig. 2, X-ray photoelectron spectra (XPS) of S 2p core level for the in situ outgassed samples revealed characteristic S $2p_{3/2}$–S $2p_{1/2}$ spin-orbital splitting. XPS analysis is useful for evaluating qualitatively the types of sulfur species and measuring quantitatively the sulfonic acid groups near the surface

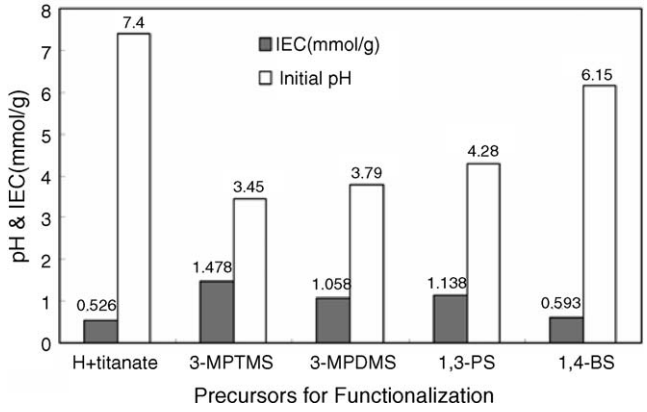


Fig. 1. pH and ion exchange capacities (IEC) of titanate nanosheets upon grafting precursors.

region. The chemical properties of the samples were probed by examining the more intense component S $2p_{3/2}$. Samples showed two types of sulfur species: one at a low binding energy (BE) (∼163.5 eV), corresponding to a sulfide ($S^{2-}$) species due to thiol (–SH) groups, and the other at a higher BE (∼168.5 eV), associated with a sulfate ($S^{6+}$) species due to sulfonic ($-SO_3H$) group [30]. Considering the intensity of $S^{6+}$ peaks in Fig. 2 for $HSO_3$-titanate samples, we can conclude that 3-MPTMS and 1,3-PS are more efficiently grafted onto the surface of titanate than 3-MPDMS and 1,4-BS. In case of 3-MPTMS as a sulfonic acid source (Fig. 2(c and d)), a large fraction of thiol group has been lost from surface during oxidation reaction with hydrogen peroxide. On the other hand, in case of 1,3-PS as a sulfonic acid source (Fig. 2(f)), a large amount of sulfonic acid group is directly grafted onto the surface of titanate. Table 1 shows the contents of sulfur in functionalized titanate quantified by

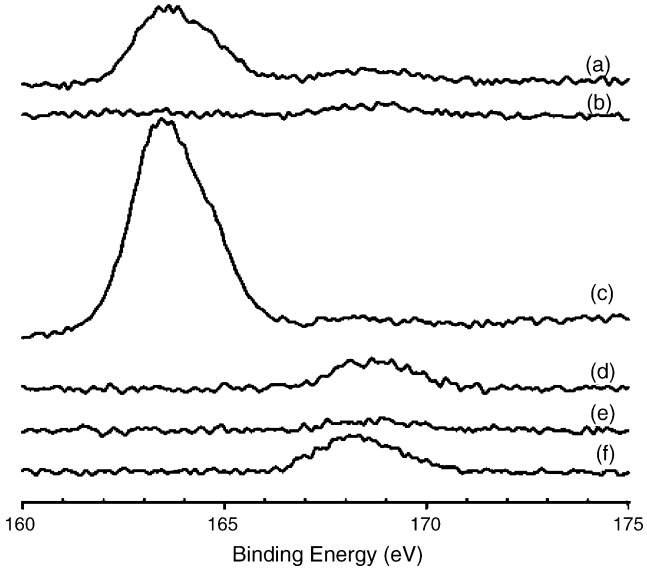


Fig. 2. X-ray photoelectron spectra (XPS) in the S 2p core level region of (a) HS-titanate (3-MPDMS), (b) $HSO_3$-titanate (3-MPDMS), (c) HS-titanate (3-MPTMS), (d) $HSO_3$-titanate (3-MPTMS), (e) $HSO_3$-titanate (1,4-BS) and (f) $HSO_3$-titanate (1,3-PS).

Table 1
Sulfur contents of functionalized titanate determined by XPS

| Sulfonic acid precursors | Sulfur contents (at%) in functionalized titanate | |
|---|---|---|
| | HS-titanate | $HSO_3$-titanate |
| Thiol | | |
| 3-MPTMS | 7.97 | 1.06 |
| 3-MPDMS | 4.21 | 0.71 |
| Sultone | | |
| 1,3-PS | – | 1.44 |
| 1,4-BS | – | 0.40 |

XPS analysis. As evident in Table 1, 1,3-PS is the most efficient reagent in grafting sulfonic acid group on titanate.

In Fig. 3, X-ray diffraction (XRD) of the functionalized titanates indicated an increase in interlayer distance by fuctionalization of surface hydroxyl (–Ti–OH) with 3-MPTMS, followed by oxidation of thiol to sulfonic acid or direct sulfonation with 1,3-PS. From the Bragg's law [31], its interlayer distance was estimated to increase from ~0.9 to ~1.0 nm, indicating that the grafted functional groups (–SH or $–SO_3H$) on surface increased slightly the interlayer distance of the titanate. This result indicates that the interlayer space of titanates has been used for functionalization. On the other hand, functionalization with 1,4-BS had little effect on the interlayer distance. This was consistent with previously described XPS results that showed a very small amount of sulfur species on the surface of this sample.

$^{29}$Si MAS NMR spectroscopy is an excellent method to study silylated compounds [32,33]. $H^+$-titanate exhibits no resonance in the range from 0 to −200 ppm as shown in Fig. 4(a). Upon surface fuctionalization with 3-MPTMS, a new broad peak (T) appeared near −50 to −70 ppm as shown in Fig. 4(b). This new peak (T) was due to the silane species grafted on the surface and in accord with the reported Si signal for alkyltrimethoxysilane or alkyltrichlorosilane grafted on layered silicates (near −55 to −65 ppm) [32,33]. Thus, the Si atom is covalently bonded to carbon forming $–O_3Si–CH_2–$ species. When HS-titanate (3-MPTMS) was treated with hydrogen peroxide to oxidize the thiol group, the intensity of new peak (T) decreased, indicating that a large portion of grafted molecules was detached from titanate surface. These results of $^{29}$Si MAS NMR are consistent with the previously described results based on XRD and XPS.

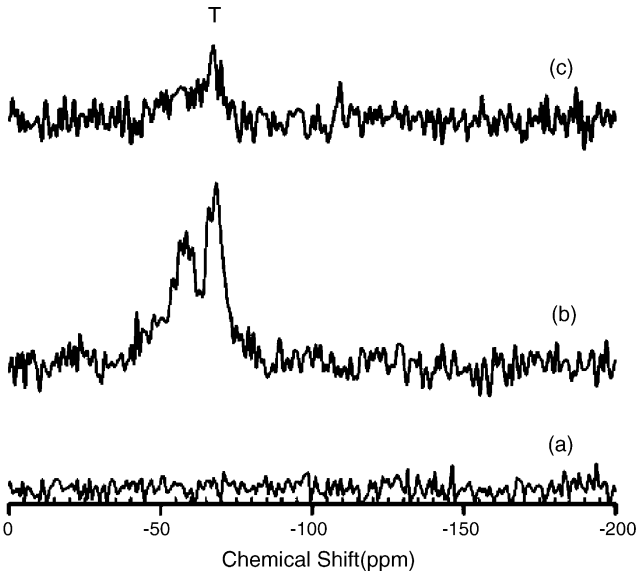


Fig. 4. $^{29}$Si MAS NMR spectra of (a) $H^+$-titanate, (b) HS-titanate (3-MPTMS) and (c) $HSO_3$-titanate (3-MPTMS) (oxidation at 333 K). The sample (c) was obtained after the protonation reaction with 1N $H_2SO_4$ at 298 K.

The thermal stability of the functionalized titanates was studied by thermogravimetric analysis (TGA) shown in Fig. 5. The weight losses of untreated, $HSO_3$-titanate (3-MPTMS) and $HSO_3$-titanate (1,3-PS) in the temperature range from 323 to 373 K were ca. 6 wt%, and probably caused by loss of water contained in inter-layers. In the case of HS-titanate (3-MPTMS), a weight loss of ca. 13 wt% was recorded between 533 and 773 K as shown in Fig. 5(b) because the surface-functionalized thiol group was thermally decomposed through this region. In case of $HSO_3$-titanate (3-MPTMS), a weight loss of ca. 6 wt% was recorded between 453 and 523 K as shown in Fig. 5(c)

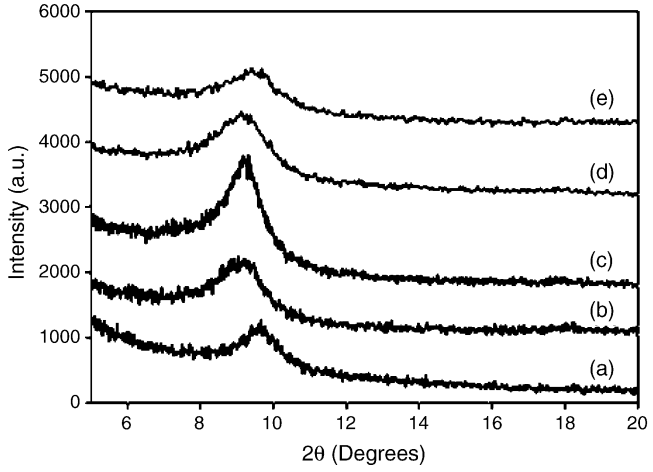


Fig. 3. Wide-angle X-ray diffraction (XRD) patterns of (a) $H^+$-titanate, (b) HS-titanate (3-MPTMS), (c) $HSO_3$-titanate (3-MPTMS), (d) $HSO_3$-titanate (1,3-PS) and (e) $HSO_3$-titanate (1,4-BS).

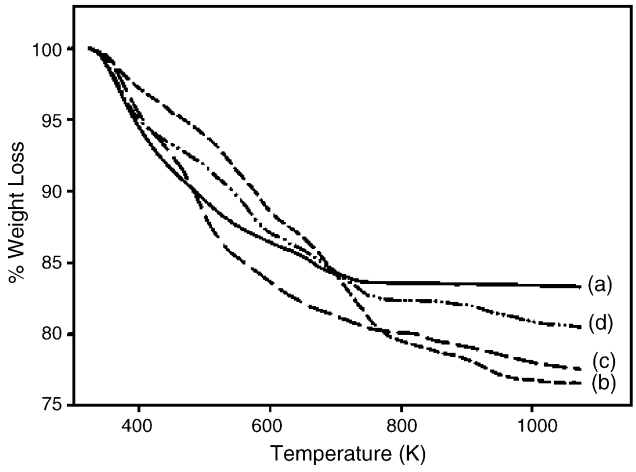


Fig. 5. Thermogravimetric analysis (TGA) curves of (a) $H^+$-titanate, (b) HS-titanate (3-MPTMS), (c) $HSO_3$-titanate (3-MPTMS) and (d) $HSO_3$-titanate (1,3-PS).

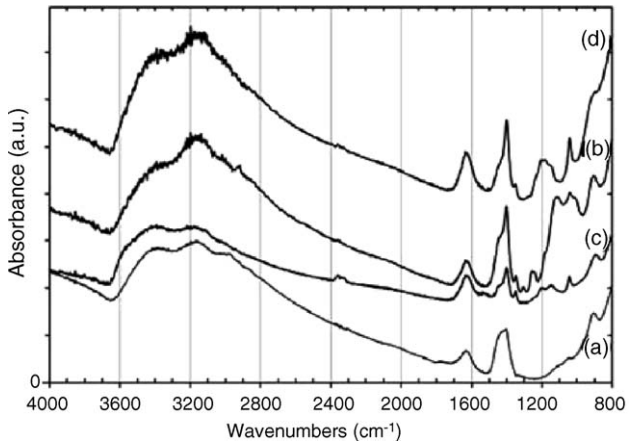


Fig. 6. Fourier transformed-infrared (FT-IR) spectra of (a) $H^+$-titanate, (b) HS-titanate (3-MPTMS), (c) $HSO_3$-titanate (3-MPTMS) and (d) $HSO_3$-titanate (1,3-PS).

because the sulfonic acid group was thermally cracked throughout this region. However, a weight loss of ca. 7 wt% was recorded between 423 and 573 K for $HSO_3$-titanate (1,3-PS) in Fig. 5(d). The sulfonic acid group grafted by using 1,3-PS had an enhanced thermal stability than that prepared using 3-MPTMS. In any case, the thermal stability of the sulfonic acid group would limit the allowed operating temperature of these materials. Fortunately, however, the decomposition temperatures are all much higher than usual operating temperatures of DMFC (<353 K).

Fig. 6 compares FT-IR spectra of thiol and sulfonic acid grafted samples. In all FT-IR spectra, the absorption bands in the range of 3600–3000 $cm^{-1}$ and near 1630 $cm^{-1}$ could be assigned to adsorbed $H_2O$ and Ti–OH coordination, respectively. The absorption band near 3400 $cm^{-1}$ results from hydroxyl group or water on the surface. In contrast, the absorption bands in the range of 1200–1000 $cm^{-1}$ in Fig. 6(b) could be due to the grafted thiol (–SH) group. Upon oxidation with hydrogen peroxide, the new absorption bands appeared at 1300–1100 $cm^{-1}$ as shown in Fig. 6(c), which is due to the grafted sulfonic acid ($–SO_3H$) group [34]. In case of grafting with 1,3-PS, the similar absorption bands at 1300–1100 $cm^{-1}$ appeared in Fig. 6(d). However, the absorption intensity of the peak for $HSO_3$-titanate (1,3-PS) was more intense than that of $HSO_3$-titanate (3-MPTMS).

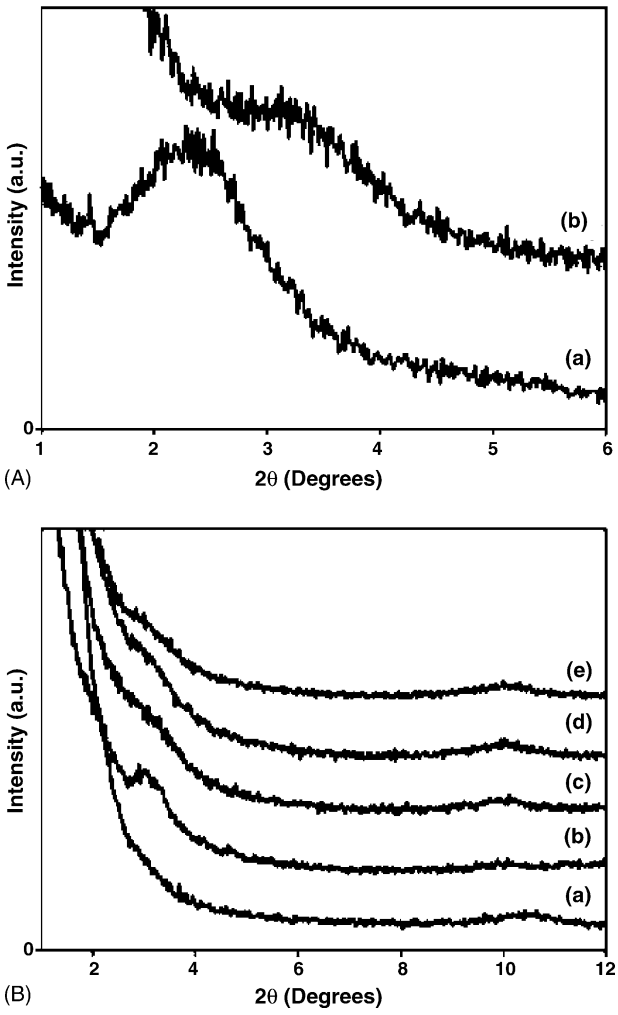


Fig. 8. Small (A) and wide-angle (B) X-ray diffraction (XRD) patterns. (A) (a) Nafion 115 membrane, (b) Nafion®/$HSO_3$-titanate (1,3-PS) nanocomposite membrane (3 wt% loaded); (B) (a) $H^+$-titanate, Nafion®/$HSO_3$-titanate (1,3-PS) nanocomposite membrane loaded amount of (b) 3 wt%, (c) 5 wt%, (d) 7 wt% and (e) 10 wt%.

### 3.2. Nafion/sulfonated titanate nanocomposite membranes

Nanocomposite membranes based on Nafion have been prepared using surface-sulfonated titanate nanosheets as inorganic

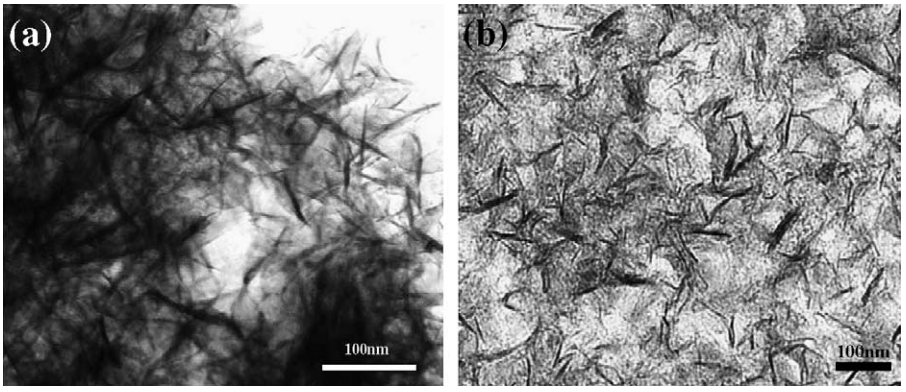


Fig. 7. Transmission electron microscope (TEM) images of (a) $HSO_3$-titanate (1,3-PS) and (b) nanocomposite membrane (3 wt% $HSO_3$-titanate (1,3-PS)).

fillers. Fig. 7 displays TEM images of $HSO_3$-titanate (1,3-PS) nanosheets without and with Nafion matrix. In Fig. 7(a), the TEM image was obtained from the samples that were prepared by dispersing the samples in ethanol using ultrasonic treatments, dropping them onto a porous carbon film supported on a copper grid and drying at 353 K in an oven. The nanosheet morphology has a thickness of ca. 10–20 nm and a width of over several hundred nanometers. After incorporating $HSO_3$-titanate (1,3-PS) into the Nafion matrix, as shown in Fig. 7(b), $HSO_3$-titanate (1,3-PS) was well dispersed in the Nafion matrix. The nanosheets became thinner in the Nafion matrix in general including some degree of exfoliation. The small-angle XRD patterns of pristine Nafion and the 3 wt% loaded nonocomposite membrane in Fig. 8(A) show a single peak that represents channel size in Nafion matrix [29]. The shift of the peak in Fig. 8(A, a) to a higher $2\theta$ angle in Fig. 8(A, b) indicates that the size of the ion channel in the nanocomposite membrane was reduced by introduction of the sulfonated titanate, relative to that of pristine Nafion. The ion channel size has a direct effect on the methanol permeability rate of the membrane. From Bragg's law [31], the ionic channel size was estimated to be reduced from 3.84 to 2.75 nm. This smaller channel in the composite electrolyte membrane could be the factor responsible for the reduced methanol crossover through the electrolyte membrane as discussed below. As shown in Fig. 8(B, a–e), as the amount of sulfonated titanate loading into the Nafion matrix was increased, the peak intensity of the small-angle region (around 3°) was decreased, which suggested that the disordering of the ion channel structure was increased. The shifts of the peak at ca. 10° to lower angles could be explained by partial intercalation of the polymer chains into the interlayer of the sulfonated titanate. This could be taken as evidence for the close interaction between Nafion and the inorganic fillers.

The tensile strength of a polymeric material has been shown to be remarkably improved when nanocomposites are formed with layered materials [35,36]. The formation of nanocomposites exhibited a large increase in the tensile properties at a rather low filler content. In the case of nanocomposites, the extent of the improvement of the modulus depended directly upon the morphology and the aspect ratio of the dispersed inorganic fillers. Fig. 9(A and B) shows the effect of the morphology. Montmorillonite (MMT) had a large particle size of micrometer scale and its aspect ratio was over 100:1. Previously we have studied surface-sulfonated MMT as an inorganic filler of the Nafion nanocomposite for DMFC applications [29]. Surface-sulfonated titanates with a nanosheet-like morphology showed a more enhanced mechanical strength than flake (MMT) or nanoparticular ($TiO_2$ P25) morphologies. The difference between titanates and MMT, both having a layered structure, may be due to the difference in the extent of exfoliation. Sulfonated titanate with ca. 0.8 nm interlayer spacing can be easily exfoliated in a Nafion matrix. Hence the final modulus of the nanocomposite membrane made from sulfonated titanate was enhanced. $TiO_2$ P25 has no layered structure and is difficult to be homogeneously dispersed in a nanocomposite membrane. Its impact on the mechanical property of membrane was similar to that of MMT. Fig. 9(C and D) shows the effect of the sulfonated titanate (1,3-PS) content. Young's modulus increased with the content of sulfonated titanate. This smooth increase in Young's modulus suggests

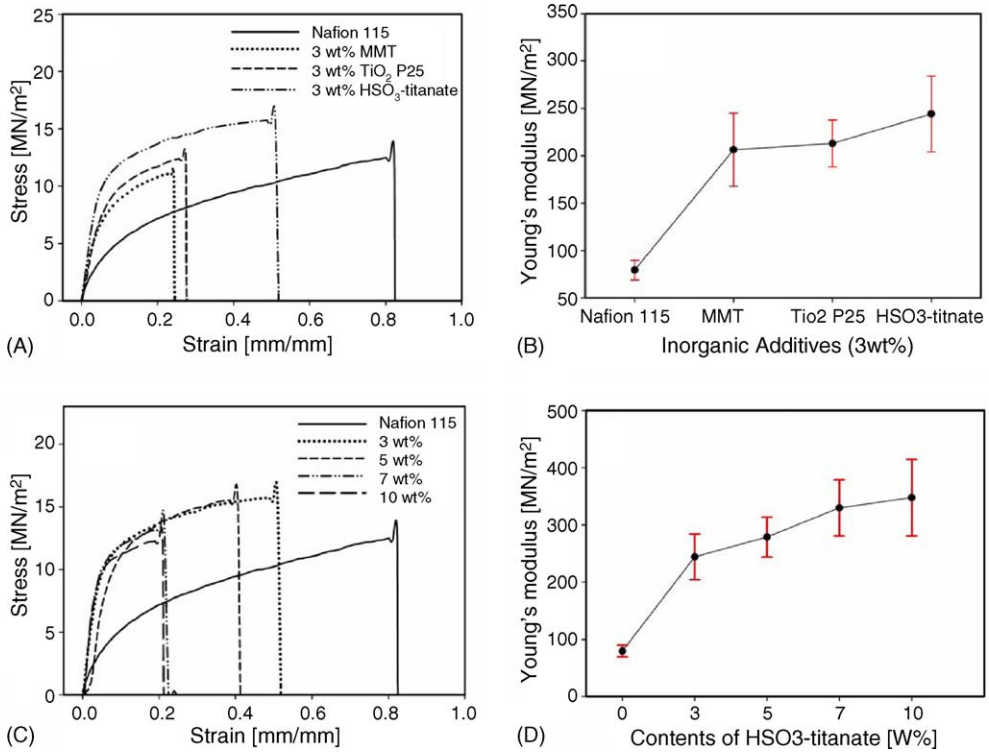


Fig. 9. Effect of morphology of inorganic fillers (A and B) and sulfonated titanate ($HSO_3$-titanate (1,3-PS)) content (C and D) on stress vs. strain and Young's modulus for nanocomposite membranes.

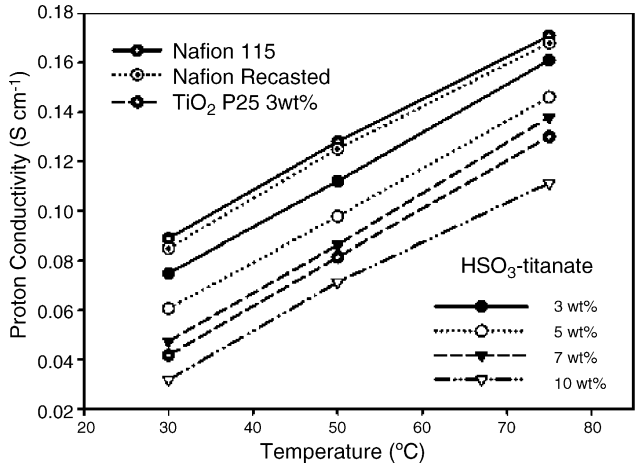


Fig. 10. The proton conductivity of Nafion 115 and nanocomposite membranes fabricated with different amounts of $HSO_3$-titanate (1,3-PS) or $TiO_2$ P25. All composite membranes had the same membrane thickness of ca. 120 μm.

fairly uniform distribution of the inorganic phase in the polymer matrix.

Fig. 10 shows the proton conductivity of membranes fabricated with different wt% of $HSO_3$-titanate (1,3-PS) (IEC ~ 1.14) in Nafion (0–10 wt%) and 3 wt% of $TiO_2$ P25. The proton conductivity of the composite membranes was measured by the ac four-point probe method using an ac impedance analyzer. Compared with the proton conductivity of Nafion 115 purchased from Aldrich, Nafion membrane recast by the solvent casting method had similar conductivity values, which shows that our preparation method is adequate for manufacturing the nanocomposite membrane. As shown in Fig. 10, the proton conductivities of nanocomposite membranes decreased with increasing the content of inorganic fillers and decreasing the measuring temperature. Nanocomposite membranes containing 3–7 wt% $HSO_3$-titanate (1,3-PS) showed higher ionic conductivity values than composite membranes containing 3 wt% $TiO_2$ P25. This trend was consistent for all three temperatures tested. These relatively higher proton conductivities of the nanocomposite membranes containing sulfonated titanates rather than the membranes containing $TiO_2$ particles are considered to be due to the effect of surface functionalization with organic sulfonic acid groups. Their conductivities are still lower than pristine Nafion membrane. Yet, the difference is smaller than the membrane containing unfunctionalized $TiO_2$, because the organic sulfonic groups on the surface contribute to the proton conduction.

Fig. 11 shows the water and methanol permeability rates of membranes fabricated with different wt% of $HSO_3$-titanate (1,3-PS) in Nafion (0–10 wt%). The thickness of the nanocomposite membranes was maintained the same at ca. 120 μm by employing the same total amount of Nafion and the inorganic filler. As shown in Fig. 11, the methanol and water permeability rates decreased with increasing the amount of $HSO_3$-titanate (1,3-PS) added into the Nafion matrix. As the concentration of methanol solution was increased, the methanol and water permeability rates proportionally increased. Table 2 summarizes the permeability properties of the nanocomposite membrane containing 10 wt% $HSO_3$-titanate (1,3-PS). The reduced permeability of

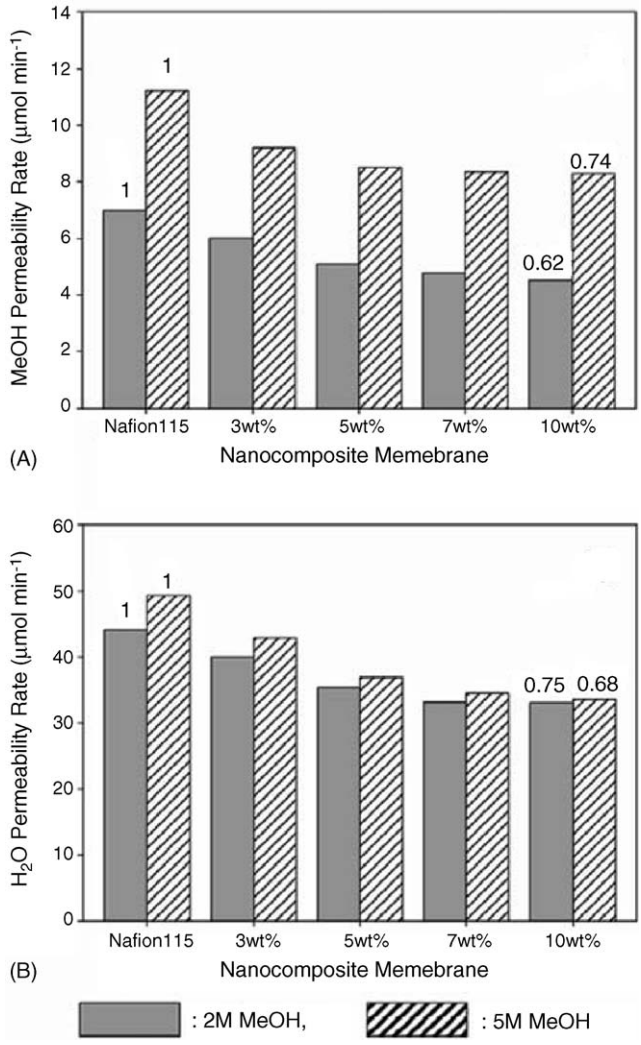


Fig. 11. The methanol (A) and water (B) permeability rates of Nafion 115 and nanocomposite membranes fabricated with different amounts of $HSO_3$-titanate (1,3-PS). All nanocomposite membranes had the same membrane thickness of ca. 120 μm. The number in figure indicates the relative permeability of methanol and water (relative to the permeability of solvent through pristine Nafion 115).

methanol was relatively large in 2 M methanol solution. Yet, the reduced permeability of water was relatively less affected by the methanol concentration.

Fig. 12 shows the performance under DMFC operating conditions of a single cell containing a membrane–electrode assembly (MEA) made with composite membranes of different inorganic materials and pristine Nafion 115. The same Pt–Ru anode and Pt cathode were employed as electrodes of the MEA. The composite membrane with 5 wt% unfunctionalized $TiO_2$ P25

Table 2
The methanol and water permeability rate of nanocomposite membrane containing 10 wt% $HSO_3$-titanate (1,3-PS)

| | 2 M MeOH | 5 M MeOH |
|---|---|---|
| MeOH | 7 → 4.5 (38%↓) | 11 → 8.3 (26%↓) |
| $H_2O$ | 44 → 33 (25%↓) | 49 → 33 (32%↓) |

*Note*: Permeability rate [μmol $min^{-1}$].

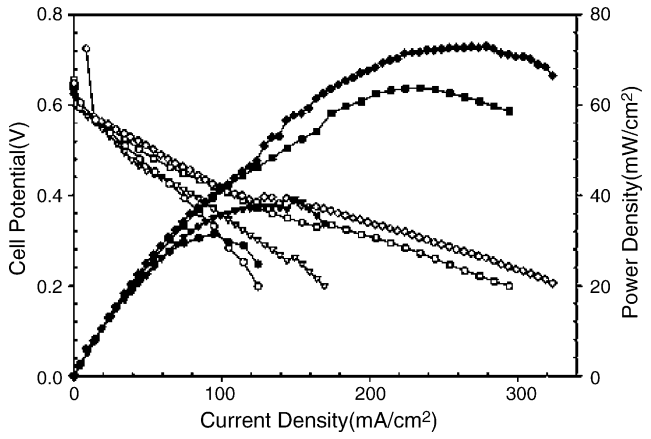


Fig. 12. Single cell performance curves for the MEA made with Nafion115 and composite membranes operated at 313 K (2 M methanol; air flow rate = 2 × stoichiometric). (●) Nafion 115, (▼) Nafion + 5 wt% unfunctionalized $TiO_2$ P25, (■) Nafion + 5 wt% $HSO_3$-titanate (3-MPTMS), (□) Nafion + 5 wt% $HSO_3$-titanate (1,3-PS).

had a better performance than Nafion 115 itself. Moreover, the composite membranes with 5 wt% functionalized titanate nanosheets showed a much improved performance compared with a composite membrane with 5 wt% unfunctionalized $TiO_2$ P25. Further, the composite membranes with 5 wt% $HSO_3$-titanate (1,3-PS) showed a higher performance than with 5 wt% $HSO_3$-titanate (3-MPTMS). The current densities measured with the composite membranes with 5 wt% inorganic fillers such as $TiO_2$ P25, $HSO_3$-titanate (3-MPTMS) and $HSO_3$-titanate (1,3-PS) were 169, 284 and 318 mA $cm^{-2}$, respectively, at a potential of 0.2 V. The current density measured with Nafion 115 was 125 mA $cm^{-2}$ at a potential of 0.2 V. Thus, the performance of the DMFC was improved by using the composite membranes, and it was much more effective to use a composite membrane containing functionalized titanates rather than unfunctionalized $TiO_2$ particles. The maximum power density of each MEA containing different membranes – Nafion 115 and the composite membranes with different inorganic fillers such as $TiO_2$ P25, $HSO_3$-titanate (3-MPTMS) and $HSO_3$-titanate (1,3-PS) – was 31.4, 39.3, 63.8 and 73.0 mW $cm^{-2}$, respectively. The maximum power density of the MEA fabricated with $HSO_3$-titanate (1,3-PS)/Nafion composite membrane was 57% higher than that of the MEA fabricated with Nafion membrane and 46% higher than that of the MEA fabricated with unfunctionalized $TiO_2$ P25/Nafion composite membrane.

As previously mentioned, there have been many attempts to improve the cell efficiency of DMFC through incorporation of inorganic moieties into the Nafion membrane [8–15]. However, there has not been much success that parallels the expectations put into these materials. Many inorganic particles have a problem of too low an ion conductivity that lowers the ion conductivity of the composite membrane to an unacceptable level. Ion-conducting inorganics such as heteropolyacids and zirconium phosphates, have also been examined without significant success either at low temperatures below 353 K, although these materials have improved performance at higher operating temperatures over 373 K. The present system of Nafion/sulfonated titanate provides encouraging results probably by two factors: (i) the relatively high ionic conductivity of $HSO_3$-titanate compared to other inorganic fillers employed previously; (ii) the 2-dimensioal morphology of titanate nanosheets that could be more effective in blocking the passage of methanol than materials of other geometries [14,15]. Indeed, Yano et al. [37] reported that the width of clay had a direct effect on the permeability of water. The longer tortuous pathways were generated by introducing a clay with a higher aspect ratio and efficiently exfoliating the layered structure, and thus the permeability of water was more effectively reduced [37,38]. The nature of the precursors had significant influence on the effectiveness of the sulfonated titanates as fillers of the nanocomposite membranes. Relative to thiol groups, sultone groups provided a simpler one-step functionalization reaction as well as better performance, and 1,3-PS was particularly effective.

## 4. Summary and conclusions

Various thiol and sultone groups were grafted onto the surface of titanate nanosheets to render organic sulfonic acid ($HSO_3$–) functionality to their surfaces. The sulfonated titanate and Nafion formed nanocomposite membranes. Based on the results of XPS, XRD and MAS NMR, 3-MPTMS and 1,3-PS were more efficient sulfonating precursors than 3-MPTMS or 1,4-BS. By surface functionalization with organic species bearing a sulfonic acid ($HSO_3$–) group, higher IEC values were obtained than untreated titanate. In a TGA experiment, $HSO_3$-titanate (1,3-PS) showed a better thermal stability than $HSO_3$-titanate (3-MPTMS). In addition, $HSO_3$-titanate (1,3-PS) was directly synthesized by a one-pot reaction without any extra oxidation step being required for thiol (–SH) groups. The functionalization of nanostructured titanate using 1,3-PS was the most efficient route showing better results than using any other precursors.

Sulfonated titanates incorporated into Nafion were well dispersed in the Nafion matrix. Nanocomposite membranes had a reduced ion channel size of 2.75 nm and the mechanical property (Young's modulus) was highly enhanced by the presence of titanate nanosheets. The performance of Nafion®/sulfonated titanate nanocomposite membranes was evaluated under DMFC operating conditions in terms of methanol permeability, mechanical properties and proton conductivity. Nanocomposite membranes containing $HSO_3$-titanate (1,3-PS) showed higher proton conductivity than composite membranes containing untreated $TiO_2$ P25. The methanol permeability of nanocomposite membranes decreased with increasing content of $HSO_3$-titanate (1,3-PS) in the nanocomposite membranes. The relative permeabilities of methanol with 2 and 5 M methanol solutions were reduced by up to 38 and 26%, respectively, relative to pristine Nafion 115. The combination of higher IEC values, enhanced mechanical/thermal properties, and reduced methanol crossover led to the enhanced the performance of DMFCs employing Nafion/sulfonated titanate nanocomposite membranes.

## Acknowledgements

This work has been supported by National Research Laboratory Program (MOST), the Research Center for Nano Catalysis (MOCIE), Hydrogen Energy R&D Center (MOST) and Bioplus Co. Ltd.

## References

[1] N.A. Hampson, M.J. Willars, B.D. McNicol, J. Power Sources 4 (1979) 191–201.
[2] X. Ren, M. Wilson, S. Gottesfeld, J. Electrochem. Soc. 143 (1996) L12–L15.
[3] S. Surampudi, S.R. Narayanan, E. Vamos, H. Frank, G. Halpert, A. LaConti, J. Kosek, G.K. Surya Prakash, G.A. Olah, J. Power Sources 47 (1994) 377–385.
[4] K. Scott, W.M. Taama, P. Argyropoulos, K. Sundmacher, J. Power Sources 83 (1999) 204–216.
[5] S. Slade, S.A. Campbell, T.R. Ralph, F.C. Walsh, J. Electrochem. Soc. 149 (2002) A1556–A1564.
[6] M.K. Avikumar, A.K. Hukla, J. Electrochem. Soc. 143 (1996) 2601–2606.
[7] C. Pu, W. Huang, K.L. Ley, E.S. Smotkin, J. Electrochem. Soc. 142 (1995) L119–L120.
[8] K.A. Mauritz, I.D. Stefanithis, S.V. Davis, R.W. Scheetz, R.K. Pope, G.L. Wilkes, H.H. Huang, J. Appl. Polym. Sci. 55 (1995) 181–190.
[9] R.V. Gummaraju, R.B. Moore, K.A. Mauritz, J. Polym. Sci. B, Polym. Phys. 34 (1996) 2383–2392.
[10] W. Apichatachuapan, R.B. Moore, K.A. Mauritz, J. Appl. Polym. Sci. 62 (1996) 417–426.
[11] P.L. Shao, K.A. Mauritz, R.B. Moore, Chem. Mater. 7 (1995) 192–200.
[12] C. Yang, S. Srinivasan, A.S. Aricò, P. Cretì, V. Baglio, V. Antonuccib, Electrochem. Solid-State Lett. 4 (2001) A31–A34.
[13] V. Tricoli, F. Nannetti, Electrochim. Acta 48 (2003) 2625–2633.
[14] D.H. Jung, S.Y. Cho, D.H. Peck, D.R. Shin, J.S. Kim, J. Power Sources 118 (2003) 205–211.
[15] J. Won, Y.S. Kang, Macromol. Symp. 204 (2003) 79–91.
[16] G. Alberti, M. Casciola, U. Costantino, M. Leonardi, Solid State Ionics 14 (1984) 289–295.
[17] G. Alberti, M. Casciola, R. Palombari, A. Peraio, Solid State Ionics 58 (1992) 339–346.
[18] G. Alberti, U. Costantino, R. Millini, G. Perego, A.R. Vivani, J. Solid State Chem. 113 (1994) 289–295.
[19] G. Alberti, L. Boccali, M. Casciola, L. Massinelli, E. Montoneri, Solid State Ionics 84 (1996) 97–104.
[20] M. Casciola, F. Marmottini, A. Peraio, Solid State Ionics 61 (1993) 125–129.
[21] P. Costamagna, C. Yang, A.B. Bocarsly, S. Srinivasan, Electrochim. Acta 47 (2002) 1023–1033.
[22] D.J.D. Corcoran, D.P. Tunstall, J.T.S. Irvine, Solid State Ionics 136–137 (2000) 297–303.
[23] J.J. Tunney, C. Detellier, Chem. Mater. 5 (1993) 747–748.
[24] E. Ruiz-Hitzky, J.M. Rojo, Nature 287 (1980) 28.
[25] T. Yanagisawa, K. Kuroda, C. Kato, React. Solids 5 (1988) 167–175.
[26] L. Merier, C. Detellier, Environ. Sci. Technol. 29 (1995) 1318–1323.
[27] C.H. Rhee, S.W. Bae, J.S. Lee, Chem. Lett. 34 (2005) 660–661.
[28] C.H. Rhee, J.S. Lee, S.H. Chung, J. Mater. Res. 20 (2005) 3011–3020.
[29] C.H. Rhee, H.K. Kim, H. Chang, J.S. Lee, Chem. Mater. 17 (2005) 1691–1697.
[30] E. Cano-Serrano, G. Blanco-Brieva, J.M. Campos-Martin, J.L.G. Fierro, Langmuir 19 (2003) 7621–7627.
[31] B.D. Cullity, Elements of X-Ray Diffraction, second ed., Addison-Wesley Publishing Company, Inc., 1978.
[32] P.H. Thiesen, K. Beneke, G. Lagaly, J. Mater. Chem. 12 (2002) 3010–3015.
[33] A. Shimojima, D. Mochizuki, K. Kuroda, Chem. Mater. 13 (2001) 3603–3609.
[34] M. Alvaro, A. Corma, D. Das, V. Fornés, H. García, Chem. Commun. 8 (2004) 956–957.
[35] S. Sinha Ray, M. Okamoto, Prog. Polym. Sci. 28 (2003) 1539–1641.
[36] N. Sukpirom, M.M. Lerner, Chem. Mater. 13 (2001) 2179–2185.
[37] K. Yano, A. Usuki, A. Okada, J. Polym. Sci. A: Polym. Chem. 35 (1997) 2289–2294.
[38] G. Alberti, M. Casciola, Annu. Rev. Mater. Res. 33 (2003) 129–154.